Proceedings of the ASME 2024
Fluids Engineering Division Summer Meeting
FEDSM2024
July 15-17, 2024, Anaheim, CA

FEDSM2024-131543

EXPERIMENTAL INVESTIGATION OF WATER DROPLET EROSION ON METALLIC AND NON-METALLIC MATERIALS

Keldon Anderson[1*], Noushin Azimy[1], Emmelia Lichty[2], Soroor Karimi[1]

[1]Department of Mechanical Engineering
University of Tulsa, Tulsa, OK
[2]Department of Mechanical Engineering
Oral Roberts University, Tulsa, OK

ABSTRACT

Water droplet erosion (WDE) is a complex phenomenon that has been investigated for nearly a century. This form of erosion affects a wide range of energy industries from steam turbines and natural gas pipelines to wind turbine blades. The moving droplets impacting at a high relative speed create a high surge in surface pressure on the impacted material and damage the surface. The damage removes materials and can compromise strength for steam turbines and pipelines or affect the lift and drag forces on wind turbine blades. Research on WDE has been ongoing for decades with a majority of the reported results focused on metallic material testing and qualitative analysis comparing methodologies or surface conditions. The ongoing research at The University of Tulsa is conducting experiments with a variety of materials while exposed to an environment where water droplet erosion occurs. Impact velocity and droplet sizes are controlled within the facility and ongoing research with particle image velocimetry (PIV) is in use to characterize the falling droplets. Stainless steel 316, Aluminum 6061, and a variety of non-metallic materials are tested for a variety of conditions. The mass of each specimen is tracked and recorded at set intervals to determine the erosion ratio and erosion rate. Various other factors such as flowrate and rotational velocity are determined before testing as well as the percentage of droplets which impact the surface is determined with the use of a high-speed camera. Scanning electron microscopy (SEM) is also utilized to examine the material's surfaces before and after testing to investigate the severity of erosion by water droplets. One impact velocity and one impact angle are set for all tested materials. These data points will be the starting point for future tests and modeling work to predict water droplet erosion based on simple factors.

Keywords: erosion, leading-edge erosion, wind turbine, droplet erosion

* Corresponding author: kla945@utulsa.edu

NOMENCLATURE

V_{drop}	droplet velocity (m/s)
V_{tip}	blade tip velocity (m/s)
V_{impact}	impact velocity (m/s)
WDE	water droplet erosion
LEE	leading edge erosion

1. INTRODUCTION

In recent years, the use of renewable sources has exceeded non-renewable sources. The global warming and environmental effects of non-renewable energies have highlighted the importance of using renewable energy resources such as wind. Wind energy has emerged as a prominent player in the field of renewable energy. As the globe struggles with climate change concerns and explores alternatives to traditional fossil fuels, the development and enhancing the efficiency of wind energy systems such as wind turbines has drawn outstanding attention [1]. One of the major parameters that affects life span and consequently the efficiency of wind turbine is erosion damages of the blades and degradation of material on them due to some effective environmental factors such as hail, dust, and rain [2]. Turbine blades are prone to erosion because of rain droplets. These rain droplet erosions reduce the turbines' life span and cause significant maintenance costs. The size of raindrops and the material of wind turbine blades both play key role on the water droplet erosion impact on wind turbines. Various research has been done on water droplet erosion and a few models have been proposed to predict such erosion but many have not been used within the industry. The majority of studies have been on metals and metallic materials. Furthermore, the influence of water droplet erosion on wind turbine blades is rarely researched [3–8].

Bech et al. [9] investigated the influence of rain droplet size on glass fiber-epoxy coated by polyurethane specimens in the erosion test at four different rain field. An experimental model for impingement to erosion as a function of drop size and impact velocity is presented. In comparison to models based on the usual

2.38-mm drop size, the drop size dependent model indicated an average 2.35 times longer durability. The study by Yamagata et al. [10] demonstrates the significance of impact velocity. They examined the aluminum's erosion performance in a pulsed-jet erosion laboratory for a wind turbine blade. According to the experimental findings, the impact velocity was around 20% lower than the nozzle departure velocity determined by the flow rate measurement. Ibrahim et al. [11] proposed an analytical model for the prediction of threshold velocity that is a crucial tool for the selection and design of materials resistant to WDE. Also, an empirical method to investigate the threshold velocity is presented. Jing et al. [12] experimentally and numerically evaluated the influence of different surface features on WDE. According to this research, for a grooved surface, a thin layer of water forms in the groove, helping to lessen the impact of ensuing water droplets, but the highest erosion is not impacted by applying these grooves.

The current study is conducting experiments with a variety of materials while exposed to an environment where water droplet erosion occurs. Each material is exposed to water droplet erosion at the same flowrate, impact angle, and impact velocity. The outcome of these tests serves as baseline for test going forward and the resulting modeling work in future studies.

2. MATERIALS AND METHODS

2.1 Testing Materials

The materials used in the oil & gas industry as well as renewable energy productions are both subjected to erosion by repeated liquid impact. Arabnejad et al. [13] presented a detailed analysis of multiple metallic materials used for pipelines and their performance when exposed to liquid impact by droplet and jet impingement. The oil & gas pipelines and various equipment have been utilizing non-metallic material in place of steel but a majority of research as to their erosion performance has been focused on solid particle impacts [14]. On the other hand, in the renewable energy sector, the wind turbine blades are composed of alternating layers of composites, bonding agents, and coatings to provide a clean, smooth surface with a solid structure that is highly flexible and has a higher strength to weight ratio than metals [15-17]. Keegan et al. [17] discussed how these layers degrade when exposed to excess heat and moisture as the protective surface layers are removed by erosion.

The materials selected for testing in this study are based on their application for both oil & gas applications and wind turbine blade construction. A total of six materials were selected for experimental testing with liquid droplet erosion at 20-m/s impact velocity. Two of the specimens are metallic materials, Stainless Steel 316 (SS316) and Aluminum 6061 (AL6061), as well as four non-metallic materials. These materials are generic High-Density Polyethylene (HDPE), Polyphenylene Sulfide (PPS), Fiberglass-Reinforced Plastic composite (FRP), and a proprietary Polyether Ether Ketone (PEEK) material. The PPS and PEEK materials do not have any form of fiber reinforcement. The material properties for both the metallic and non-metallic specimens are listed in Table 1. The specimens are cut into a rectangular shape with dimensions of 50x38-mm with varying thickness from 2-mm to 10-mm. The surfaces of the materials were not ground to a uniform finish, so the surface tested is as machined or formed by the manufacturer.

TABLE 1: MATERIAL CODENAMES AND PROPERTIES OF TESTED SPECIMENS

Material Name	Code	Hardness Rockwell A (Shore D)	Density (g/cc)
Aluminum 6061	AL6061	50	2.7
Stainless Steel 316	SS316	80	9
Polyether Ether Ketone	PEEK	(90)	1.1
Polyphenylene Sulfide	PPS	(90)	1.5
Fiberglass-Reinforced Plastic	FRP	(85)	1.8
High Density Polyethylene	HDPE	(90)	0.9

Several of the tested non-metallic materials are known to have moisture absorption up to 0.5% of their body weight, yielding an average mass gain of 10-mg. This absorbed moisture can affect material properties as discussed by Bibhardt et. al. for FRP as well as Faria et. al. for PPS [18,19]. The methodology for understanding the observed mass change of the specimen during testing is detailed in section 2.3.

2.2 Testing Apparatus

The facility follows the ASTM G73 testing standard used for a rotating testing apparatus for liquid impingement erosion testing [20]. A multitude of facilities exist to test liquid impact erosion via high-speed impact, but their respective purpose and application varies widely. Many of these facilities follow the G73 standard, however, the variation of facilities creates difficulty when comparing results and testing applications. Reported results also vary as a significant portion of those results are published as comparison between materials, a single variable, or a combination of the two [3,21]. Nash et al. conducted an interesting test where an FRP type material was coated in an unlisted leading edge coating system and then exposed to WDE for various lengths of time. Their objective was to give a timeline analysis of the erosion phases for this material at a single velocity. Their results supported the original idea of a long incubation period where no erosion occurs then changes to rapid mass loss in a shorter period of time [22]. Valaker et al. is also conducted WDE tests on coated material but they conducted test on aluminum disks with various coatings. These samples were exposed to a single impact velocity for 30 and 60 min where the coatings were analyzed after to determine percentage of removal and mass loss [23].

These results are beneficial when handled in an enclosed environment, such as deciding which material is better, but the lack of recording other values proves troublesome when

comparing facilities and test replication. The most common version of these facilities is via a whirling arm testing apparatus where the specimen is rotated at a high rate in an artificial rain field. These facilities often record mass change of the specimens based on the artificial environmental conditions and adjustable variables such as impact velocity, impact angle, and droplet size [20–23]. Figure 1 shows a general schematic of the facility used at the University of Tulsa [29].

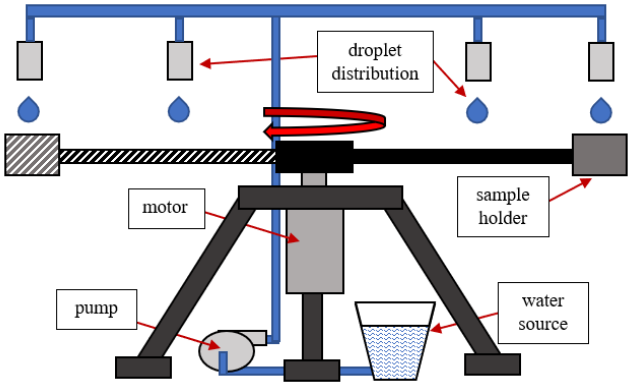

FIGURE 1: SCHEMATIC OF LIQUID DROPLET FACILITY AT UNIVERSITY OF TULSA [29].

A new facility, installed at the University of Tulsa, consists of a concrete room housing the whirling arm testing apparatus. This facility follows the aforementioned ASTM G73 standard and will replicate previous experiments in literature as well as conducting additional experiments for several specimens and conditions. Figure 2 shows the interior of the facility with the rotating arms and artificial rain field source shown. The rotating arms are powered by a Dayton 10-hp (7.5kW), 3-phase electric motor controlled by a variable frequency drive (VFD) rated for 10-hp 3-phase motors. A mounted tachometer is installed to ensure the desired speed is reached. The VFD and tachometer reading is positioned on the exterior of the facility allowing safe access while the facility is operating. The dual 1-m long arms are composed of 25-mm SS316 with an aluminum and SS316 airfoil shell attached to the rods. The detachable samples holders are shown in Figure 2 with a specimen of HDPE attached. The exposed frontal area of the specimen is 35x50-mm and is positioned so that the specimen's surface is perpendicular to the falling droplets' direction and has minimal clamping and bending force on the material.

The artificial rain field is created via 5 droplet stations positioned along the swept perimeter of the specimen's path. Each station has two, 3D-printed devices that have an interchangeable blunt needle attached. The needles are a consistent internal diameter with a known droplet size produced when water is pumped throw the needle. Figure 2 also shows the needle holder with a 14-gauge (1.6-mm ID) needle installed and a sleeve that covers the needle to minimize exposure from any wind that the facility creates. One peristaltic pump (24V DC powered, 9.6-L/h max flowrate) is installed on the exterior wall for each droplet station. The pump's electrical is connected in series to a control box to have precise control of the flowrate. Each pump's flowrate is recorded at the needle source to verify that the desired flowrate is reached and within 5% difference between pumps. The adjustable flowrate and swappable needles allow the facility to have precise control over the created droplet size and frequency to be produced. Tap water is the working fluid and is stored in an outdoor, 175-gallon (650 liter) tank with individual feedlines to each pump with 65-micron filters in place to remove any particles. A diaphragm pump is placed on the exterior of the facility with the intake along the floor of the chamber and serves as a drain pump.

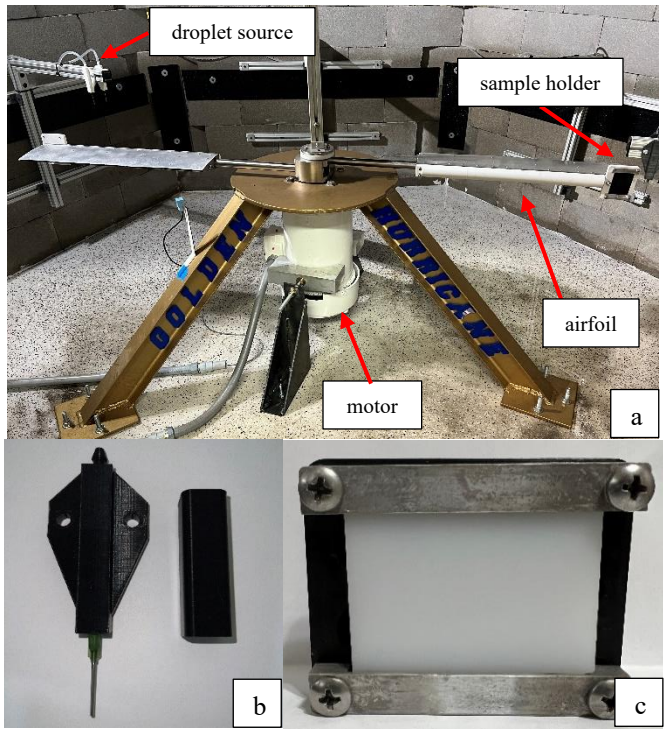

FIGURE 2: (a) IMAGE OF CURRENT LIQUID DROPLET FACILITY DEVELOPED AT UNIVERSITY OF TULSA, (b) WITH NEEDLE HOLDER AND RAIN SHIELD, AND (c) CURRENT SAMPLE HOLDER.

2.3 Experimental Method

The facility is properly secured for all connection points and the desired impact angle is set via rotating the central rod then the high strength bolts are torqued to specifications. The facility is then powered on and the tachometer, VFD, and pumps are inspected and verified to be operating within acceptable conditions.

The selected specimen's weight is recorded with an Ohaus AX324 electronic mass balance with a 320g capacity and 0.1mg resolution. Each specimen is weighed a minimum of 5 times to determine a stable average and standard deviation. Due to the experiment's measuring point being longer than 24-hours, a 10-g calibrated weight is also weighed to establish a historical accuracy of the scale. Once a neutral mass is recorded, the specimen is then placed in an oven at 70°C to remove any

absorbed moisture. This process is required for testing non-metallic materials as the material type tends to absorb moisture at a rate that can affect mass readings after erosion testing. Each material has a predetermined time to be placed in the oven concluding a water absorption test following the ASTM D570 standard [30]. This test involves weighing the specimen for an initial weight then submerged in water for 24-hours then weighed to record the percentage of body weight the specimen absorbed. Following the 24-hour absorption and weigh in, the specimen is then placed in the 70°C oven for a minimum of 24 hours then weighed. This process of drying then weighing is repeated till the average is within 0.3mg difference across two consecutive days. The testing specimens are then placed in the facility and secured to the sample holder with the aluminum brackets. The specimen is secured with minimum force to prevent any excess loading across the specimen as that has been noted to affect erosion [25].

The droplet sources are aligned to the center of the specimen with a slight offset towards the center to adjust for the movement of the droplets during operations. This droplet movement while falling is estimated to be 10mm in the radial direction and 15mm in the tangential direction. This deflection has been observed previously and measured in the facility via GoPro video. The desired needle size is installed, and the shield is attached to all the droplet stations. The droplet size is calculated utilizing particle image velocimetry (PIV) with the produced droplet diameters, velocity, and circularity having been predetermined and connected to needle gauge size. The pumps can be turned on and then adjusted to reach the set flowrate and measured to confirm the position. Flowrate is verified to be consistent between each needle station and adjusted as required.

The PIV systems contains a dual-pulse laser system measuring velocity and droplet size in a 2D plane. A modified replica of the droplet production system has the produced droplets falling in the laser field for observation. Due to the high reflectivity of droplets, a fluorescent dye is added to the water at 3% concentration by volume to aid in image processing. A total of 250 pairs of images, with hundreds of droplets captured, were used for data processing. The results from PIV concluded that the droplets have an average velocity of 1.2-m/s so their influence on impact velocity is negligible and only decreases as tip velocity increases.

Once the specimens have been prepared and the droplet sources are at the desired flowrate, the facility can be fully secured, and the motor can start. The VFD controls the motor by adjusting the input frequency to vary the rotational speed. A conversion table for RPM to tip velocity (m/s) is placed alongside the VFD and tachometer readout to verify that the facility has reached operational condition. The impact velocity is determined by Eqn. 1 where the tip velocity and falling droplet velocity are summed together.

$$V_{impact} = V_{tip} - (-V_{drop}) \quad (1)$$

Erosion rate and erosion ratio are the two primary values calculated and reported for erosion testings as they provide a baseline comparisons between materials and simple conditons. Erosion rate is defined as the total mass loss of the sample divided by the total exposure time to erosion. Erosion ratio is the total mass loss of the sample divided by the total mass of the impacting fluid. A factor is required to correct the amount of droplets produced into the amount that impacted the specimen. This factor is termed the strike factor, SF, and is simply the percentage of created droplets that impact the sample and is a function of pump flowrate, system RPM, and needle size. Strike factor is determined thru the use of high speed videography and assuming that all droplets are close to the same size and have identical mass. For all the materials tested at 20-m/s with a total flowrate of 24 L/hr the strike factor was found to be 32% of the droplets produced would impact the specimen. With the strike factor and erosion rate known, the erosion ratio can be determined.

3. RESULTS AND DISCUSSION

The materials listed in Table 1 were tested at 20-m/s impact velocity for a minimum of 96 hours of exposure to water droplet impacts. The largest droplet size, determined through PIV analysis briefly mentioned earlier, that impacted the specimen is 3.5-mm at a constant flowrate of 4.8 L/h per pump station. Results were based on hundreds of sets of images taken from falling droplets and analyzing their diameter and velocity.

Figures 3 and 4 below show the results for Aluminum 6061 material and serve as a reference to the expected results of a material tested under erosion. Figure 3 tracks the daily mass change of each AL6061 (Al#1 and Al#2) specimen along with the 10-g calibrated weight (CW). Each measurement point is collected from weighing the sample a minimum of five times and then averaged. The graph indicates that the mass loss is consistent between each measurement point which is expected as the testing conditions were held constant. The positive values of AL6061 indicate that mass loss via erosion is present and the materials absorb any moisture at an insignificant amount.

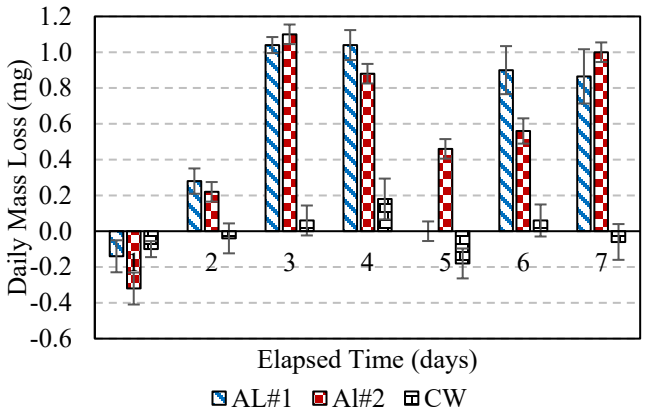

FIGURE 3: DAILY MASS LOSS OF Al6061 AGAINST ELAPSED TIME DURING WDE TESTING.

The cumulative daily mass loss is shown in Figure 4 against cumulative experimental exposure time. The data on each graph

contains data points collected when pre-drying the specimen, during WDE testing, and drying the specimen after WDE exposure has concluded. For plots where the cumulative mass loss is plotted against time, the calibrated weight is not included as the data points would only lie on the horizontal axis. SS316 and Al6061 were not dried before WDE tests as they show no history of water absorption. All data points for graphs where cumulative mass loss is plotted against exposure time contain error bars based on the standard deviation between measurement points.

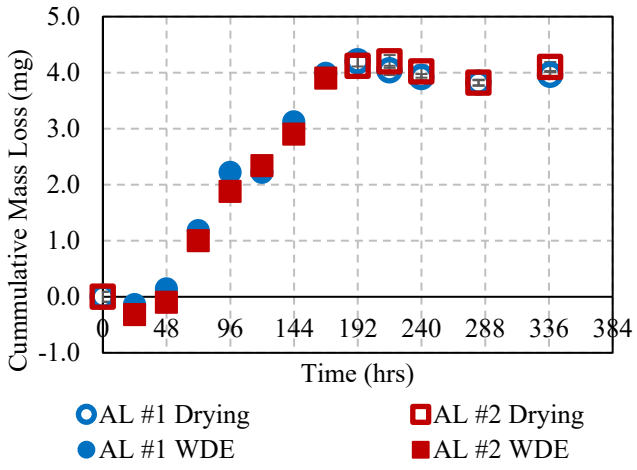

FIGURE 4: CUMULATIVE MASS LOSS OF Al6061 MATERIAL (168-HRS WDE EXPOSURE).

Figures 5-10 show the cumulative mass loss of PEEK, PPS, FRP, HDPE, and SS316 respectively during WDE and drying period (before and after WDE tests where applicable). Table 2 presents the total mass loss, erosion rate (g/hr), erosion ratio (g/g), and erosion ratio (mm^3/mm^3) for all materials tested. The results for PEEK, PPS, and FRP have an initial observed mass gain during testing followed by a steady mass loss as the samples were removed and placed in an oven to dry.

The results for SS316 and HDPE, in Figures 5 and 6 respectively, provide two issues with the current testing practices with these materials. SS316 yielded no measurable mass loss as the recorded values oscillated within the error of the scale. HDPE showed signs of moisture absorption, noted in the mass gain during testing and mass loss when drying, which was not known prior to testing. For future tests with SS316, test velocity will need to be increased or test duration increased to expedite erosion or go beyond the incubation period for the material. For HDPE, all non-metallic materials, regardless of prior history to low moisture absorption, will be dried prior to testing and afterwards to record only mass loss due to erosion.

PPS and PEEK (Figures 7 and 8 respectively) are the only materials to have a sample size of one. These materials shared similar absorption values so were chosen to be tested at the same time. Future plans include testing these two materials again to ensure repeatability. The drying weight is included for both materials before and after WDE testing. As expected, the materials have a noticeable amount of moisture absorbed from the local environment and is removed steadily over time inside the oven. This moisture is then reintroduced during testing and once again removed afterwards.

Results for FRP are split between Figures 9 and 10 due to the large amount of moisture absorbed during testing. Figure 10 shows an apparent mass gain after 400 hours, possibly due to abnormally high ambient humidity due to local weather, which the samples absorbed rapidly while mass was being recorded. This effect was observed while each sample rested on the scale where their weight rose at a steady rate within seconds. As expected, the cumulative mass loss trend varies greatly between the material types while the deviation between the pair of tested specimens remains consistent and minimal.

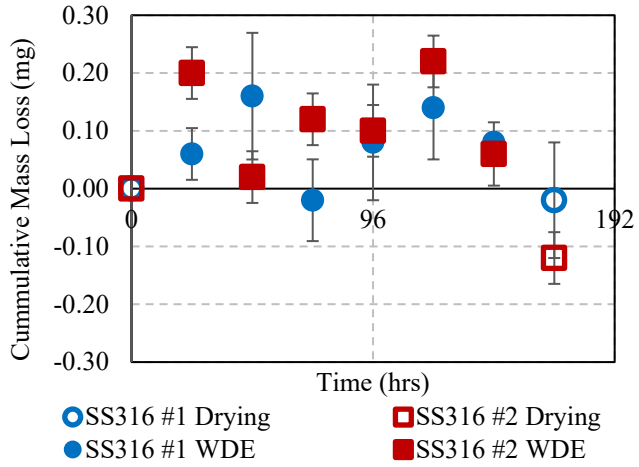

FIGURE 5: CUMULATIVE MASS LOSS OF SS316 MATERIAL (144-HRS WDE EXPOSURE).

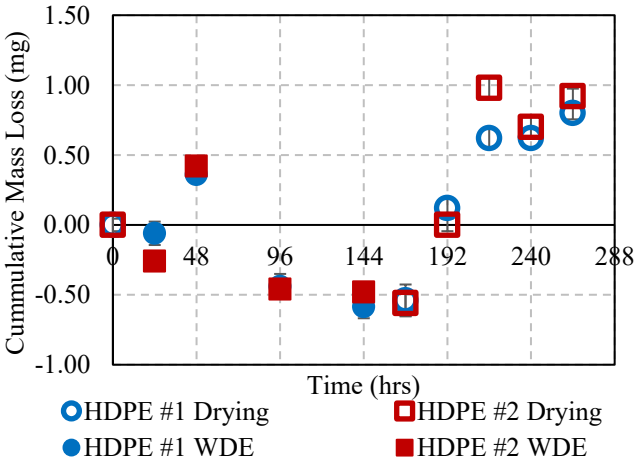

FIGURE 6: CUMULATIVE MASS LOSS OF HDPE MATERIAL (144-HRS WDE EXPOSURE).

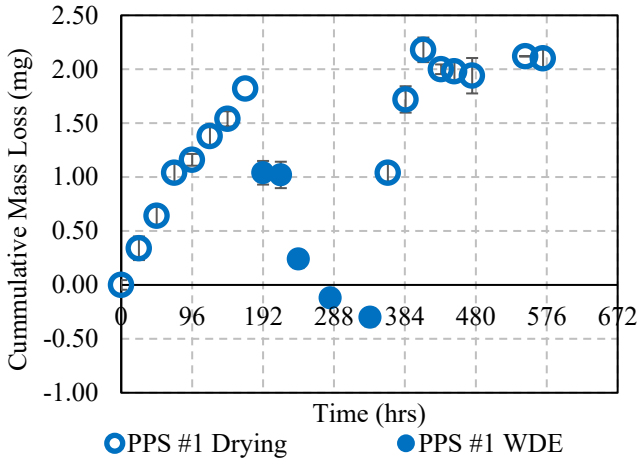

FIGURE 7: CUMULATIVE MASS LOSS OF PPS MATERIAL (168-HRS WDE EXPOSURE).

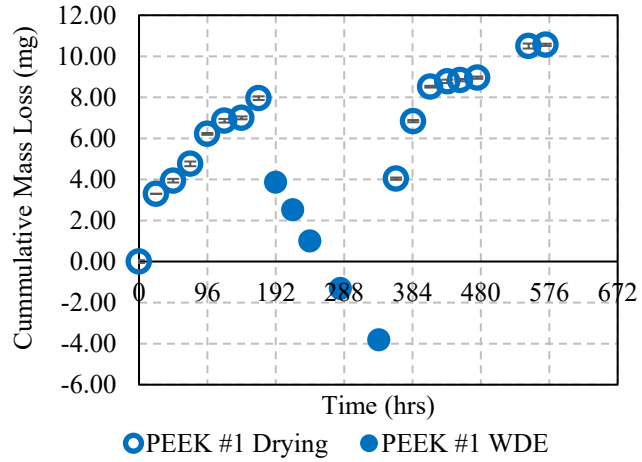

FIGURE 8: CUMULATIVE MASS LOSS OF PEEK MATERIAL (168-HRS WDE EXPOSURE).

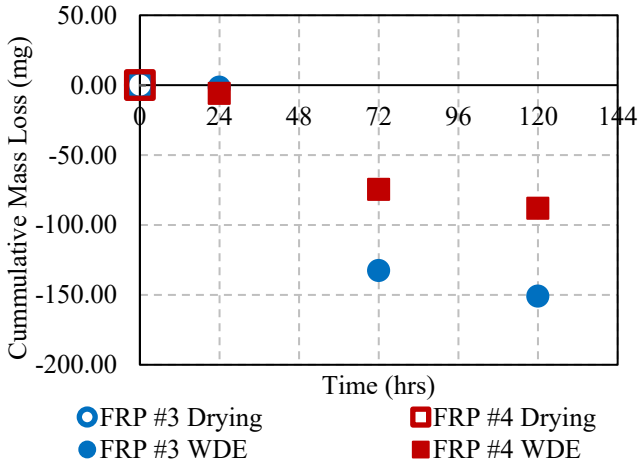

FIGURE 9: CUMULATIVE MASS LOSS OF FRP MATERIAL (120-HRS WDE EXPOSURE).

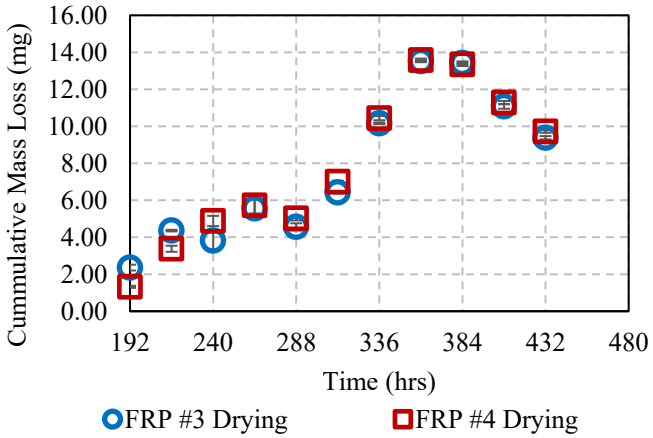

FIGURE 10: CUMULATIVE MASS LOSS OF FRP MATERIAL (120-HRS WDE EXPOSURE).

The calculated average erosion results are listed in Table 2 for all materials. The mass loss is calculated as the initial value after pre-drying the specimen and the final value after drying for a measured period after erosion testing. The lengths of drying and erosion testing time is typically 1:1, meaning that 7 days of testing require 7 days of drying before and again after testing. As previously mentioned, the erosion rate is the ratio of the total mass change of the sample by the total erosion exposure time and the erosion ratio is the ratio of the total mass change of the sample by the total erosion impacting fluid multiplied by the strike factor. The erosion ratio is presented in both g/g for a mass loss ratio and in mm3/mm3 for the volume loss ratio. The results collected serve as an example of the complexity and challenges that are faced for water droplet erosion on non-metallic materials as the moisture absorption continues to offer a challenge. Figure 11 contains the mass loss data for all materials when exposed to WDE at the same conditions (20-m/s impact velocity at 90-degrees with droplet flowrate at 4.8-L/h with 14 gauge needles). The vertical axis is split to allow the results for FRP to be viewed alongside the other materials. This figure aids in showing the difference between how non-metallics and metals react when exposed to WDE conditions.

TABLE 2: EROSION RESULTS FOR VARIOUS SPECIMENS

Material	Mass Loss (mg)	Erosion Rate (g/hr)	Erosion Ratio (g/g)	Erosion Ratio (mm^3/mm^3)
AL6061	4.0	2.40E-05	3.12E-09	1.16E-09
SS316	-0.1	-4.86E-07	-6.33E-11	-7.03E-12
PPS	0.8	4.85E-06	6.32E-10	4.21E-10
HDPE	0.9	5.97E-06	7.78E-10	8.64E-10
PEEK	4.1	2.44E-05	3.17E-09	2.65E-09
FRP	9.6	7.96E-05	1.04E-08	5.45E-09

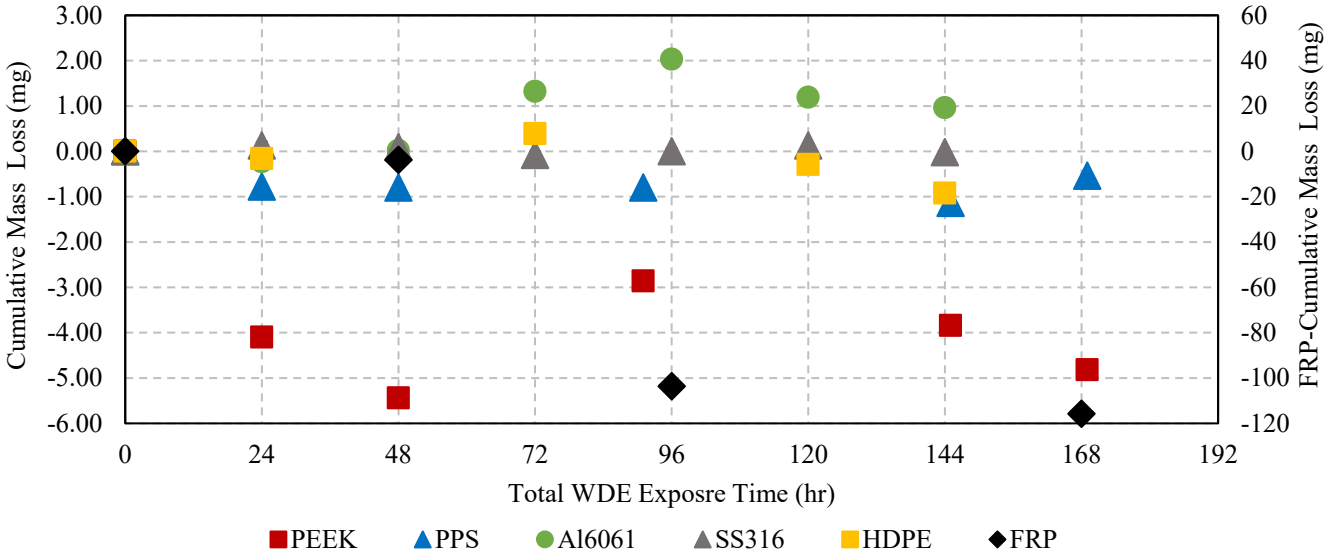

FIGURE 11: CUMULATIVE MASS LOSS VERSUS WDE EXPOSURE TIME FOR ALL MATERIALS.

The average erosion ratio for Al6061 at 20-m/s is 3.12E-09 g/g with a standard deviation of 7.67E-11 g/g. The average standard deviation for the other materials is 7.03E-11 g/g, calculated from the two specimens tested for HDPE and FRP. The value for standard deviation is acceptable as the value is determined only from two values and there is a natural instability of erosion testing and measurement.

Scanning electron microscopy (SEM) results are shown in Figures 12-17 for the area directly exposed to erosion and the outer edge of the sample where droplets did not impact the surface to represent the un-eroded or control surface. Figure 12 shows the specimen for AL6061 after WDE testing with the "eroded" and "control" regions defined. At small magnification (Figure 13) the surface difference between the eroded and control areas is minimum but higher magnification images for AL6061 tests are shown in Figure 14. The higher magnification in the eroded area highlights a multitude of indentations caused by repeated droplet impact, with an example circled in red. Figure 15 shows the SEM results for SS316 after being exposed to droplet erosion at 20-m/s impact velocity for 144 hours. The surface shows a minor texture difference when the eroded area is observed. The surface grains are more apparent after erosion exposure but no signs of significant damage is shown. This minor change in topography shows promise that the erosion can be quantified via mass loss when higher impact velocities are tested. Figure 16 shows the SEM results for PEEK after being exposed to droplet erosion at 20-m/s impact velocity for 168 hours. The surface of the material has "scars" on both the control surface and the eroded area but is much more prominent. The black markings were observed across the whole surface of the specimen and is likely due to the sputter coating used for SEM images of non-metallics. The surface damage is noticeable but is not as severe as what is observed with aluminum which is to be expected as Al6061 has lower strength and surface hardness.

Lastly, Figure 17 shows the SEM images for PPS after 168 hours of WDE exposure. Surface pitting is noted across the material surface but the largest of which is noted in the region where droplets directly impacted the specimen. No other signs of damage was noted and the material did not have any supporting fibers which may have shown more obvious signs of damage. SEM imagery for the remaining materials, as well as other specimens and test conditions, are planned for future work.

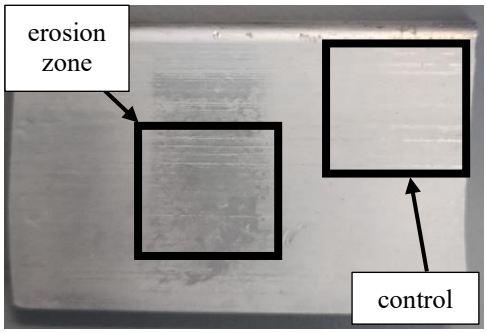

FIGURE 12: TESTED SPECIMEN FOR AL6061 WITH EROSION AND CONTROL SECTIONS OUTLINED FOR SEM.

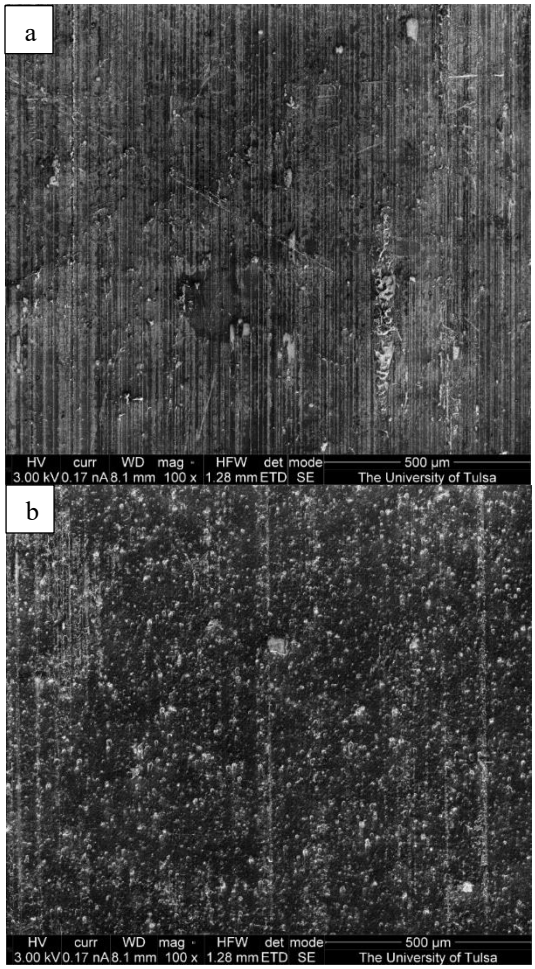

FIGURE 13: SEM RESULTS FOR AL6061 (a) CONTROL AND (b) ERODED AREAS AT LOW MAGNIFICATION.

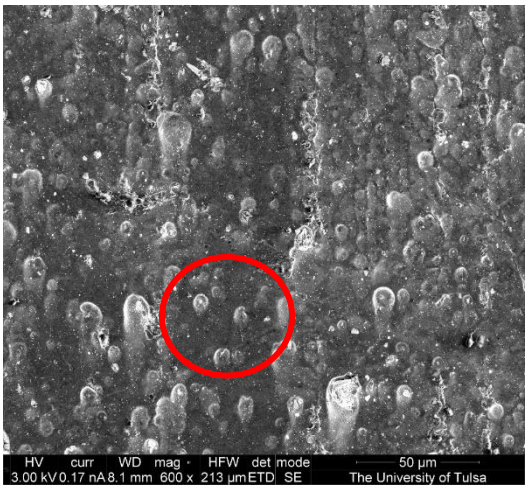

FIGURE 14: SEM RESULTS FOR AL6061 AT ERODED AREA WITH NOTICEABLE IMPACT INDENTATIONS**.**

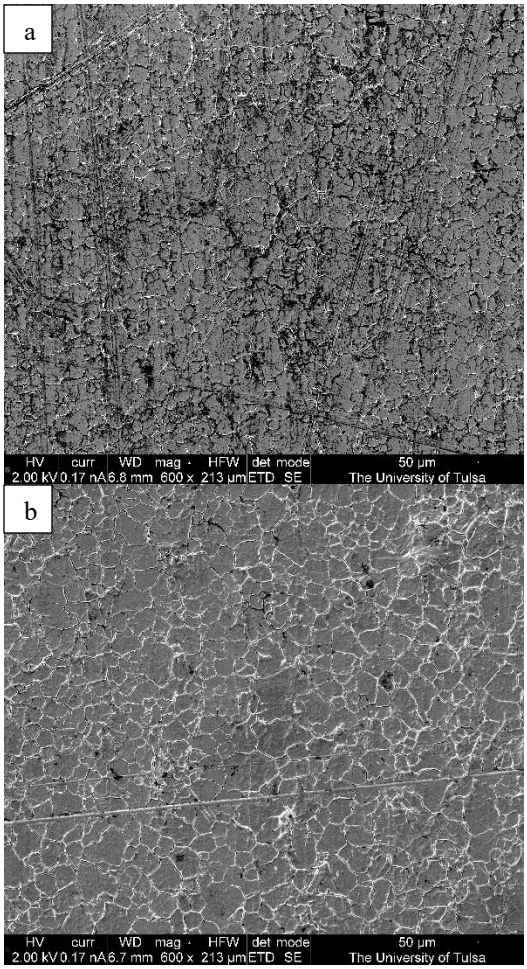

FIGURE 15: SEM RESULTS FOR SS316 (a) CONTROL AND (b) ERODED AREAS.

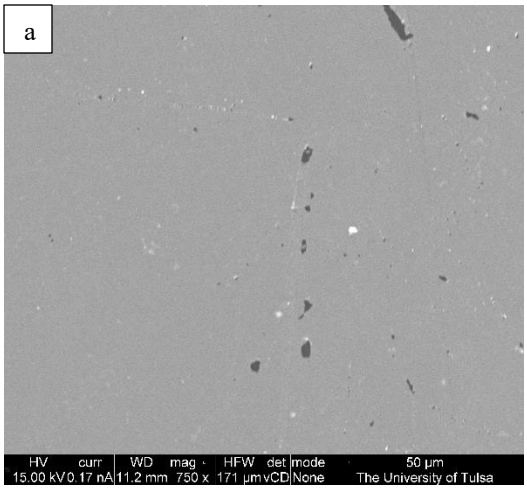

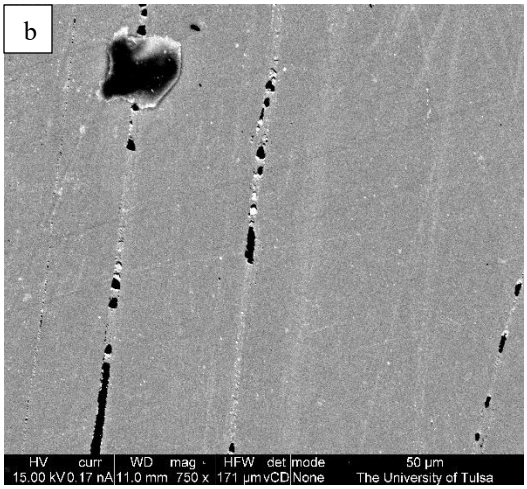

FIGURE 16: SEM RESULTS FOR PEEK (a) CONTROL AND (b) ERODED AREAS.

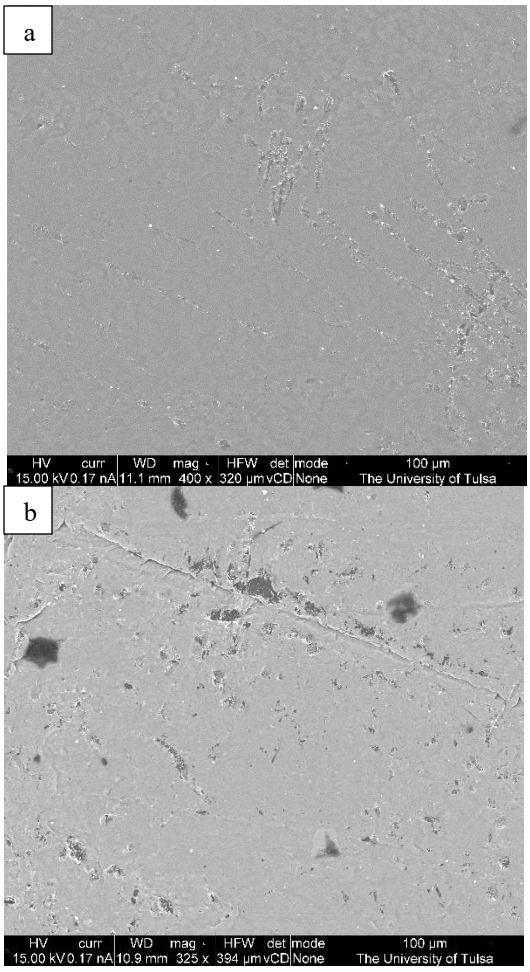

FIGURE 17: SEM RESULTS FOR PPS (a) CONTROL AND (b) ERODED AREAS.

4. CONCLUSION AND FUTURE WORK

The experimental work done to analyze and quantify liquid impact erosion has been ongoing for decades with interest primarily focused on metallic materials. However, the application of this decades long research on non-metallic materials is unknown and the concern of its validity grows year after year as complex materials, like those used in wind turbine blades, are being utilized more and more. The University of Tulsa has conducted tests on metallic materials in the past for liquid jet impact and has developed a new facility for testing droplet impact on a variety of materials. The currently tested materials, two metallic and four non-metallics, indicated that their droplet erosion resistance properties vary drastically between one another. The complexity of testing non-metallics has been made apparent with the noticeable amount of moisture absorption during testing and the ambient absorption when samples have been dried. Further testing with the new facility, not just for more materials but other erosion conditions, will yield a generalized erosion model that can predict erosion caused by liquid droplet impacts. The application of this model will aid the design work done for many industries such as oil & gas pipeline operations and wind turbine designs.

ACKNOWLEDGEMENTS

The authors would like to acknowledge and thank Hayden Wheeler for his help with maintaining the facility and assisting in modifications. The authors would also like to acknowledge the NSF REU grant number 1852477 and Dr. Laura Ford for supporting the undergraduate student Emmelia Lichty on her research of PIV study of falling droplets.

REFERENCES

[1] Slot, H. M., Gelinck, E. R. M., Rentrop, C., and Van der Heide, E., 2015, "Leading Edge Erosion of Coated Wind Turbine Blades: Review of Coating Life Models," Renew Energy, **80**, pp. 837–848.

[2] Verma, A. S., Castro, S. G. P., Jiang, Z., and Teuwen, J. J. E., 2020, "Numerical Investigation of Rain Droplet Impact on Offshore Wind Turbine Blades under Different Rainfall Conditions: A Parametric Study," Compos Struct, **241**(January).

[3] Fujisawa, K., Ohki, M., and Fujisawa, N., 2019, "Influence of Surface Roughness on Liquid Droplet Impingement Erosion," Wear, **432–433**(February).

[4] Tobin, E. F., Young, T. M., Raps, D., and Rohr, O., 2011, "Comparison of Liquid Impingement Results from Whirling Arm and Water-Jet Rain Erosion Test Facilities," Wear, (271), pp. 2625–2631.

[5] Valaker, E. A., Armada, S., and Wilson, S., 2015, "Droplet Erosion Protection Coatings for Offshore Wind Turbine Blades," Energy Procedia, **80**, pp. 263–275.

[6] Kirols, H. S., 2015, "Water Droplet Erosion: Influencing Parameters, Representation and Comparisons," Concordia University Montreal,.

[7] Domenech, L., García-Peñas, V., Šakalyte, A., Francis, D. P., Skoglund, E., and Sánchez, F., 2020, "Top Coating Anti-Erosion Performance Analysis in Wind Turbine Blades Depending on Relative Acoustic Impedance. Part

2: Material Characterization and Rain Erosion Testing Evaluation," Coatings, **10**(8), pp. 1–20.
[8] Kirols, H. S., Kevorkov, D., Uihlein, A., and Medraj, M., 2015, "The Effect of Initial Surface Roughness on Water Droplet Erosion Behaviour," Wear, **342–343**, pp. 198–209.
[9] Bech, J. I., Johansen, N. F. J., Madsen, M. B., Hannesdóttir, Á., and Hasager, C. B., 2022, "Experimental Study on the Effect of Drop Size in Rain Erosion Test and on Lifetime Prediction of Wind Turbine Blades," Renew Energy, **197**(June), pp. 776–789.
[10] Yamagata, T., Hasegawa, M., and Fujisawa, N., 2023, "Erosion Behavior of Pulsed-Jet Test Facility for Wind Turbine Blade," **515**(July 2022).
[11] Ibrahim, M. E., and Medraj, M., 2022, "Materials & Design Prediction and Experimental Evaluation of the Threshold Velocity in Water Droplet Erosion," Mater Des, **213**, p. 110312.
[12] Jing, M., Gujba, A. K., and Medraj, M., 2022, "Experimental and CFD Simulation of Interactions between Water Droplets with Different Surface Features to Understand Water Droplet Erosion," **586**, pp. 573–586.
[13] Arabnejad, H., Mansouri, A., Shirazi, S. A., McLaury, B. S., and Shadley, J. R., 2015, "Erosion-Corrosion Study of Oil-Field Materials Due to Liquid Impact," NACE - International Corrosion Conference Series, pp. 1–8.
[14] Anderson, K., Karimi, S., and Shirazi, S., 2021, "Erosion Testing and Modeling of Several Non-Metallic Materials," Wear, **477**(March), p. 203811.
[15] Engel, O. G., 1958, "Erosion Damage to Solids Caused by High-Speed Collision with Rain," J Res Natl Bur Stand (1934), **61**(1), p. 47.
[16] Mishnaevsky, L., Branner, K., Petersen, H. N., Beauson, J., McGugan, M., and Sørensen, B. F., 2017, "Materials for Wind Turbine Blades: An Overview," Materials, **10**(11), pp. 1–24.
[17] Keegan, M. H., Nash, D. H., and Stack, M. M., 2013, "On Erosion Issues Associated with the Leading Edge of Wind Turbine Blades," J Phys D Appl Phys, **46**(38).
[18] Gibhardt, D., Doblies, A., Meyer, L., and Fiedler, B., 2019, "Fatigue and Mechanical Properties of Glass Fibre Reinforced Epoxy," Materials, **7**(55), p. 23.
[19] Faria, M. C. M. D., Appezzato, F. C., Costa, M. L., Oliveira, P. C. D., and Botelho, E. C., 2011, "The Effect of the Ocean Water Immersion and UV Ageing on the Dynamic Mechanical Properties of the PPS/Glass Fiber Composites," Journal of Reinforced Plastics and Composites, **30**(20), pp. 1729–1737.
[20] ASTM G73-10, 2012, "Standard Test Method for Liquid Impingement Erosion Using Rotating Apparatus," ASTM Book of Standards: G73-10.
[21] Zhang, Z., Zhang, D., and Xie, Y., 2019, "Experimental Study on Water Droplet Erosion Resistance of Coatings (Ni60 and WC-17Co) Sprayed by APS and HVOF," Wear, **432–433**(May).
[22] Nash, D., Leishman, G., Mackie, C., Dyer, K., and Yang, L., 2021, "A Staged Approach to Erosion Analysis of Wind Turbine Blade Coatings," Coatings, (11).
[23] Valaker, E. A., Armada, S., and Wilson, S., 2015, "Droplet Erosion Protection Coatings for Offshore Wind Turbine Blades," Energy Procedia, **80**, pp. 263–275.
[24] Groucott, S., Pugh, K., Zekos, I., and Stack, M. M., 2021, "A Study of Raindrop Impacts on a Wind Turbine Material: Velocity and Impact Angle Effects on Erosion Maps at Various Exposure Times," Lubricants, **9**(6).
[25] Pugh, K., Rasool, G., and Stack, M. M., 2019, "Raindrop Erosion of Composite Materials: Some Views on the Effect of Bending Stress on Erosion Mechanisms," J Bio Tribocorros, **5**(2), pp. 1–12.
[26] Siddons, C., Macleod, C., Yang, L., and Stack, M., 2015, "An Experimental Approach to Analysing Rain Droplet Impingement on Wind Turbine Blade Materials," European Wind Energy Association Annual Conference and Exhibition 2015, EWEA 2015 - Scientific Proceedings.
[27] Mackie, C., Nash, D., Boyce, D., Wright, M., and Dyer, K., 2019, "Characterisation of a Whirling Arm Erosion Test Rig," 2018 Asian Conference on Energy, Power and Transportation Electrification, ACEPT 2018, pp. 1–2.
[28] Nash, D., Leishman, G., Mackie, C., Dyer, K., and Yang, L., 2021, "A Staged Approach to Erosion Analysis of Wind Turbine Blade Coatings," Coatings, (11).
[29] Anderson, K., Karimi, S., and Shirazi, S., 2022, "Development of Droplet Erosion Testing Facility," Fluid Engineering Division, pp. 1–6.
[30] Klyosov, A. A., 2007, "Wood-Plastic Composites," Wood-Plastic Composites, **16**, pp. 1–698.